Strumpellin and Spartin, Hereditary Spastic Paraplegia Proteins, are Binding Partners

Jiali Zhao[1] and Peter Hedera[1,2]

[1]Department of Neurology, [2]Center for Molecular Neuroscience, Vanderbilt University, Nashville, TN, USA.

ABSTRACT: Hereditary spastic paraplegia (HSP) is one of the most heterogeneous neurodegenerative diseases with more than 50 identified genes causing a relatively stereotypical phenotypic presentation. Recent studies of HSP pathogenesis have suggested the existence of shared biochemical pathways that are crucial for axonal maintenance and degeneration. We explored possible interactions of several proteins associated with this condition. Here we report interactions of endogenous and overexpressed strumpellin with another HSP-associated protein, spartin. This biochemical interaction does not appear to be a part of the Wiskott–Aldrich syndrome protein and Scar homologue (WASH) complex because spartin is not co-immunoprecipitated with WASH1 protein. The spartin–strumpellin association does not require the presence of the microtubule interacting and trafficking domain of spartin. Overexpression of mutant forms of strumpellin with the introduced HSP-causing mutations does not alter the colocalization of these two proteins. Knockdown of strumpellin in cultured cortical rat neurons interferes with development of neuronal branching and results in reduced expression of endogenous spartin. Proteosomal inhibition stabilized the levels of spartin and WASH1 proteins, supporting increased spartin degradation in the absence of strumpellin.

KEYWORDS: strumpellin, spartin, hereditary spastic paraplegia, WASH complex

CITATION: Zhao and Hedera. Strumpellin and Spartin, Hereditary Spastic Paraplegia Proteins, are Binding Partners. *Journal of Experimental Neuroscience* 2015:9 15–25 doi:10.4137/JEN.S22969.

RECEIVED: December 17, 2014. **RESUBMITTED:** April 6, 2015. **ACCEPTED FOR PUBLICATION:** April 10, 2015.

ACADEMIC EDITOR: Lora Talley Watts, Editor in Chief

TYPE: Original Research

FUNDING: Authors disclose no funding sources.

COMPETING INTERESTS: Authors disclose no potential conflicts of interest.

CORRESPONDENCE: peter.hedera@vanderbilt.edu

Paper subject to independent expert blind peer review by minimum of two reviewers. All editorial decisions made by independent academic editor. Upon submission manuscript was subject to anti-plagiarism scanning. Prior to publication all authors have given signed confirmation of agreement to article publication and compliance with all applicable ethical and legal requirements, including the accuracy of author and contributor information, disclosure of competing interests and funding sources, compliance with ethical requirements relating to human and animal study participants, and compliance with any copyright requirements of third parties. This journal is a member of the Committee on Publication Ethics (COPE).

Published by Libertas Academica. Learn more about this journal.

Introduction

Hereditary spastic paraplegia (HSP), also known as Strumpell–Lorraine disease, is a group of neurodegenerative disorders that are characterized by relatively isolated axonal degeneration, resulting in fairly uniform clinical and pathological phenotype. HSP is genetically very heterogeneous with more than 50 causative genes identified.[1] This suggests the existence of several shared biochemical pathways playing roles in the pathogenesis of HSP, and their elucidation may provide further insights into the basic cellular pathways required for axonal maintenance or axonal degeneration.[2]

HSP can be classified genetically according to the mode of inheritance, or clinically based on the presence of additional neurologic and systemic signs.[3] HSP is classified as pure (or uncomplicated) when only spastic paraparesis is present, and complex (or complicated) when additional neurological signs, such as ataxia, amyotrophy, optic nerve atrophy, or parkinsonism, are also a part of the phenotype.[4] HSP linked to chromosome 8q24, designated as SPG8, is a prototypical pure HSP with an autosomal dominant mode of inheritance.[5] It is caused by several missense mutations in the *KIAA0196* gene, encoding a protein of 1,159 amino acids, namely, strumpellin.[6] This is a highly conserved protein with a relative paucity of identified functional domains, including a spectrin-repeat-containing domain within amino acids 434–518 and an alpha-helix from amino acids 606 to 644. The most common disease-causing mutations N471D and V629F are positioned within these conserved regions. However, the physiologic function of strumpellin and the mechanism how point missense mutations in this gene causes axonal degeneration are only emerging. Strumpellin is known to be a part of the Wiskott–Aldrich syndrome protein and Scar homologue (WASH) complex, playing a role in endosome-to-Golgi retrieval.[7,8]

Here we expand the number of known strumpellin partners by identifying the interactions with another HSP-associated protein, spartin, causing SPG20. This form of HSP is also known as Troyer syndrome, and it is classified as autosomal recessive complicated HSP.[9] It has been mostly described in an inbred Old Amish Order population, and the affected individuals suffer from spastic paraplegia associated with a mild developmental delay, distal amyotrophy, and a short stature.[9] This gene encodes a protein with 666 amino acid residues, which is ubiquitously expressed both within the nervous system and also in nonneuronal tissues.[10] The homozygous frame-shift mutation in exon 4 of spartin was found in all affected individuals, resulting in protein truncation by 268 residues.[11] Bioinformatic analysis of spartin identified a strong sequence similarity between the C-terminal region of spartin and a number of uncharacterized plant proteins associated with senescence.[11] Additionally, spartin also contains a microtubule interacting and trafficking (MIT) domain in the amino terminal region of the protein. This MIT domain

is found in a number of proteins, including the endosomal protein VPS4, which has a well-defined role in intracellular protein trafficking.[3,12] The precise function of the plant-related senescence domain remains unknown. This domain of spartin interacts with cardiolipin localized in outer mitochondrial membrane and mitochondrial cytolosol. Depletion of spartin resulted in depolarization of the mitochondrial membrane, suggesting that plant-related senesce domain of spartin is important for the regulation of mitochondrial calcium homeostasis.[13] Spartin is a multifunctional protein with several known functions, including regulation of lipid droplet biogenesis by promoting AIP4-mediated ubiquitination of several lipid droplet proteins, epidermal growth factor receptor trafficking, and an inhibitor of the bone morphogenic signaling pathway.[11,14–16] Our work also suggests that the spartin–strumpellin interaction takes place outside the WASH complex, further supporting additional functions of strumpellin.

Experimental Procedure

Eukaryotic DNA expression constructs. The full length of spartin:myc and deletion constructs spartin 1–208:myc, which contains the MIT domain, and spartin 208–666:myc, which contains the plant-senescence-related region, were a gift from Dr. Blackstone.[11] The full coding sequence of the *KIAA0196* gene (accession number NM_014846) was amplified from the human brain tissue using 5′-ATGTTGGACTTTC-TAGCCGAG-3′ and 5′-AACTACTCAAGTCTTGTCAC-GACATT-3′ primers. The polymerase chain reaction (PCR) product was verified by sequencing and cloned into the eukaryotic expression vector of pEGFP-N2 at NheI and KpnI restriction sites to generate in-frame N-terminal green fluorescence protein (GFP) tagging and at Xho1 and EcoR1 restriction sites to generate in-frame C-terminal GFP tagging. The generated in-frame fusions of the strumpellin-GFP gene at both C- and N-termini were then verified by sequencing. We also generated hemagglutin (HA) epitope C-terminus tagged strumpellin and an untagged strumpellin construct, which were cloned into the eukaryotic expression vector pcDNA3.1 using Xho1 and BamH1 restriction sites. Site-directed mutagenesis was performed on GFP-tagged constructs, as described previously, and all sequences were verified.[17] Constructs containing other analyzed genes, including spastin, atlastin, NIPA1, REEP1, and paraplegin, were generated as described previously.[17,18]

Cell lines and transfection. COS7 cells, HEK-293T cells, and primary rat neuronal cultures and transfection were performed as described previously.[17,18] HEK-293 T and COS7 cell lines were purchased from American Type Culture Collection (ATCC, Manassas VA), cultured in Dulbecco's Modified Eagle's medium (Sigma-Aldrich, St. Louis, MO) containing 10% fetal bovine serum, 2 mM L-glutamine, 1 mM sodium pyruvate, 100 IU/mL penicillin, and 100 µg/mL streptomycin (Invitrogen, Carlsbad, CA), and maintained at 37°C in humidified 5% CO_2/95% air. Cells were seeded at moderate density (~50–60% confluent) in 12-well plates, and transfected the next day with the respective combination of constructs using FuGENE 6 (Roche Diagnostics, Indianapolis, IN) according to the manufacturer's protocol. The primary cortical neurons, prepared from embryonic day-18 (E18) rat embryos, were electrically transfected with the respective constructs using the nucleofactor 1 device and the manufacturer's optimized protocol for the rat neuron nucleofactor kit (Amaxa Inc., Gaithersburg, MD).[17,18] All procedures for the generation of cultured embryonal rat neurons were performed using protocols approved by the Vanderbilt University Institutional Animal Care and Use Committee.

Immunocytochemistry and confocal microscopy. Strumpellin (C-14, sc-87442) and spartin (D-4, sc-271888) antibodies were purchased from Santa Cruz Biotechnology, and WASH1 (ab157592), early endosomal antigen 1 (ab2900), and alpha-1 GABA (ab94585) antibodies were from Abcam. Specificity of strumpellin antibodies was checked by depletion of rat strumpellin using the siRNA oligonucleotides 5′-CAAAGATTCAAGACTGGCAAA-3′ cloned into pGFP-V-RS plasmid with eGFP reporter. As a negative control we used plasmid-A (sc-108060), encoding a scrambled shRNA sequence that does not affect any cellular message. Cell sorting with 2×10^6 cells selected, immunocytochemistry, semiquantitative neuronal branching assessment, and microscopy were performed as previously reported.[17,18] Cells were fixed with 4% paraformaldehyde (Electron Microscopy Sciences, Fort Washington, PA), blocked with 2% bovine serum albumin in 1 × PBS containing 0.5% Triton X-100, and incubated with the specific antibody at a dilution of 1:800. After two hours of incubation, cells were washed twice with 1 × PBS and incubated with the secondary antibody conjugated to Cy2, Cy3, or Cy5 for one hour. After three washes, coverslips were mounted onto microscope slides and fluorescent images acquired with a Zeiss LSM510 META laser-scanning confocal microscope and processed with the LSM Image software. The transfected cells were evaluated in a blind fashion with regard to the presence of wild type (WT), mutant forms, or sham transfections; we evaluated between 50 and 100 cells for each construct, and specific numbers can be found in the Results section. Images were obtained using the confocal microscope, and the LSM images were photographed at 20×, 40×, 60×, and 100× magnification.

Neuronal branching of transfected rat cortical neurons was analyzed 48 hours and 14 days after transfection. Primary and secondary neuronal dendritic branches in neurons stained with microtubule-associated protein 2 antibodies (MAP2-A4, Santa Cruz Biotechnology) were counted in a blind fashion to the transfected construct, and 100 cells for each construct were analyzed. We compared the total sum of both primary and secondary branching. The number of observed branches was compared using an unpaired Student's *t*-test.

Immunoprecipitation and Western blot analysis. For immunoprecipitation of endogenous proteins, rat brain tissue lysates were prepared from adult Wistar male rat brain using protein A/G agarose beads (Thermo Scientific), as previously described.[17,18] Western blot analysis of transfected neurons, including RNAi experiments, was done only after selection of transfected neurons by flow cytometry.[17] For immunoprecipitation of endogenous proteins, rat brain tissue lysates were prepared from adult Wistar male rat brain. The brain tissue was homogenized in M-PER protein extraction reagent (Pierce) with the protease inhibitor cocktail (Roche). The lysate was then centrifuged at 15000 rpm at 4°C for 10 minutes. The supernatant was either incubated with 6 µg of anti-strumpellin antibodies or the same concentration of control IgG derived from the same species, and 30 µL protein A/G agarose beads containing IgG binding domains of both protein A and G (Thermo Scientific) at 4°C overnight. The beads were washed by the wash buffer, and the proteins were resolved by SDS-PAGE and immunoblotted with specific antibodies. For immunoprecipitation of expressed tagged proteins, cos-7 cells were transfected as described above. After 36 hours of transfection, cells were lysated and immunoprecipitation was done as described above. Cell lysates were used as protein input control of IP, together with actin immunoblotting as a loading control. Western blot analysis of transfected neurons, including RNAi experiments, was done only after selection of the transfected neurons by flow cytometry. Samples were run on an LSR II flow cytometer (BD Biosciences), and 48 hours after transfection cell sorting was performed in which 2×10^6 GFP-positive cells were selected for each tested condition and control experiments. All experiments involving the use of multiple antibodies were done using the same membrane that was serially stripped of previous antibodies. Each experiment was repeated at least five times to verify the reproducibility of results.

Rat spartin and strumpellin protein depletion by siRNA expression. Four different siRNA oligonucleotides targeting rat spartin were designed: (1) 5′-TCCTGATAGGTCACC AGTTCTCAAGTGCA-3′, (2) 5′-GGCACACTCTCCT TGAGGACTACCAGATC-3′, (3) 5′-ATCGTGCCTTGT GAGCCGAGTTCAGAAGA-3′, and (4) 5′-GCCTCGCC ACTTCTCTACGGAATGACCTT-3′. Rat strumpellin targeting was done using siRNA oligonucleotides 5′-CAAAG ATTCAAGACTGGCAAA-3′ cloned into pGFP-V-RS plasmid with eGFP reporter. As a negative control for both experiments we used plasmid-A (sc-108060), encoding a scrambled shRNA sequence, which will not lead to the specific degradation of any cellular message. The transfected neurons were sorted flow-cytometrically, lysed, and analyzed by western blotting, as previously described.[16,17] The efficacy of spartin or strumpellin protein depletion was tested 48 hours after transfection. We performed cell sorting by flow cytometry, and 2×10^6 GFP-positive cells were selected for each tested siRNA and control experiments. The cells were lysed, and western blot with strumpellin and spartin antibodies was performed as described above to confirm knockdown of both targeted proteins. Proteosomal inhibition before western blotting was done using the MG-132 (carbobenzoxy-Leu-Leu-leucinal) inhibitor (Sigma-Aldrich, St. Louis, MO). Transfected cells were treated for six hours at 10 µM concentration before cell sorting and western blot analysis.

Quantitative R-T PCR of spartin mRNA. Total RNA was extracted from transfected neurons expressing after cell sorting procedure using the RNeasy Mini kit (Qiagen, Germantown, MD). First-strand cDNA synthesis was performed using the SuperScript III First Stand Synthesis System kit (Invitrogen, San Diego, California). Quantitative PCR itself was performed using the SYBR Green mix (QuantiTect SYBR Green PCR Kit, Qiagen). We used previously published spartin cDNA PCR primers 5′-CTGGAA ATTCTAGAGAAGGGTCTTGC-3′ and 5′-TTGTAGC ATTGTATCAGGAAACATGTAG-3′.[19] β-Actin was used as internal control. Differences in mRNA levels were assessed by a two-standard-curves method. The standard curve was the Ct value plotted against the log of the input mRNA concentration at five 10-fold serial dilutions.

Results

Strumpellin and spartin are binding partners. We explored possible interactions of strumpellin with other proteins associated with HSP, especially those playing putative roles in endosomal trafficking. First, we determined the specificity of available polyclonal anti-strumpellin antibodies because a lysate of cultured rat neurons detected multiple bands, including the expected 137-kD band. Knockdown of strumpellin using RNAi in cultured rat cortical neurons after flow-cytometric selection of GFP-positive neurons showed the disappearance of 137- and 70-kD bands, while control experiments after RNAi using nonsensical shRNA did not differ from untreated rat neuronal tissue (Fig. 1A). Western blots with anti-spartin antibodies have yielded similar results in previously published reports.[14] We also determined the specificity of anti-strumpellin antibodies for immunocytochemistry (Fig. 1B and C). Knockdown of strumpellin almost completely abolished staining in neuronal processes, even though we still observed nonspecific background in neuronal bodies.

Immunoprecipitation experiments from whole rat brain demonstrated that strumpellin and spartin interact because both proteins could be pulled down when the other putative binding partner was used as a bait (Fig. 2A and B). We observed a low-intensity nonspecific background when strumpellin was used as a bait in the third lane, which contained only A/G agarose beads with IgG binding domains of both protein A and G alone and without specific strumpellin antibodies (Fig. 2B, lane IP-IgG), but the intensity of immunoprecipitated protein was more than 100-fold higher (panel B, the second lane with anti-strumpellin antibodies). We used an unrelated

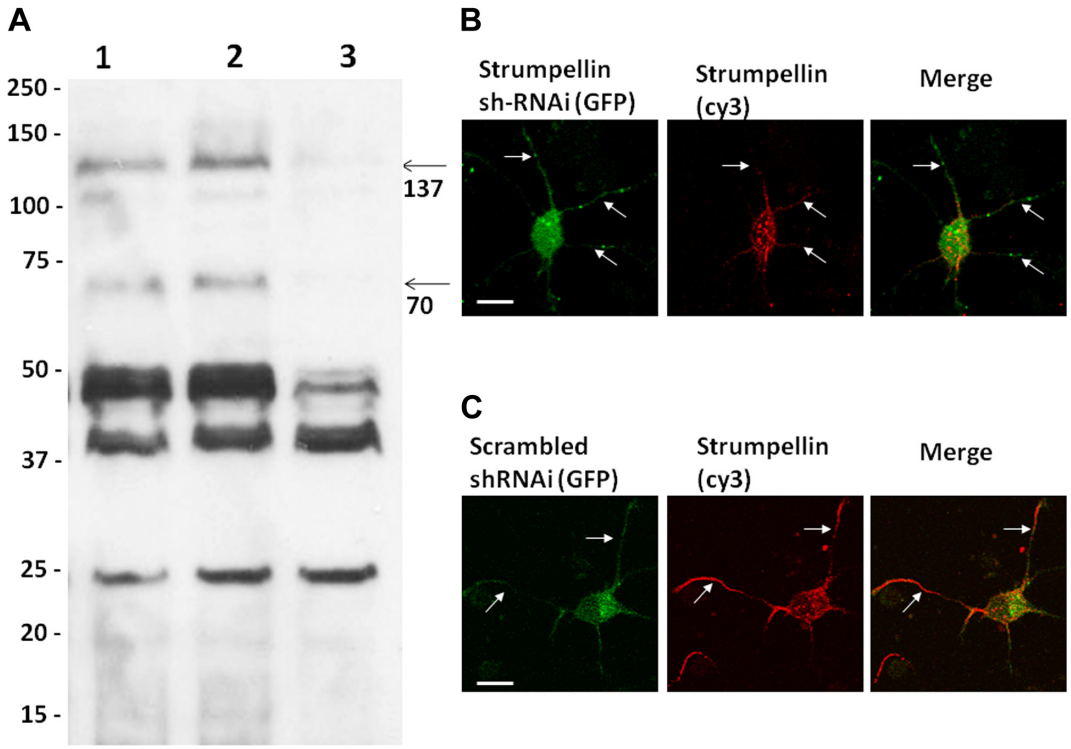

Figure 1. Specificity of polyclonal anti-strumpellin antibodies and expression pattern of endogenous and expressed strumpellin. Panel A shows western blot of rat brain homogenate using polyclonal anti-strumpellin antibodies (lane 1) with several identified bands, including the expected size of 137 kD, corresponding to a full-length strumpellin protein. The specificity of this band was confirmed by RNAi experiments targeting this transcript. The 137- and 70-kD bands disappeared (lane 3), while control experiments after RNAi using nonsensical shRNA (lane 2) did not differ from the untreated brain homogenates (lane 1). Panel B shows immunocytochemistry experiments using the same RNAi construct, which almost completely eliminated strumpellin staining from the neuronal processes (arrows), but we observed a nonspecific background in neuronal bodies. Control experiments with nonsensical shRNA transfection did not change strumpellin staining (panel C). Scale bar = 10 μm.

membrane protein, the $GABA_A$ receptor α1 subunit, as a negative control. Neither protein could be immunoprecipitated using anti-$GABA_A$ receptor α1 antibodies, further supporting the specificity of the interaction between strumpellin and spartin. Additionally, strumpellin is a known part of the WASH complex, while spartin has not been identified as its member. We were able to detect WASH1 protein interaction only with strumpellin, and spartin did not bind to WASH1 protein (Fig. 2C, the second lane). The detected nonspecific bands did not differ in their intensity among different lanes, confirming the equal loading amount of the used antibodies. Thus, WASH1 also serves both as a positive and negative control to further confirm that the detected co-immunoprecipitation of strumpellin and spartin was not due to a nonspecific interaction. We did not detect any putative interactions of strumpellin with the other analyzed proteins spastin, atlastin, NIPA1, REEP1, and paraplegin (data not shown).

Overexpressed strumpellin and spartin colocalize. Analysis of interactions of mutant forms of strumpellin and spartin required the construction of tagged constructs for both proteins. Expression of both C-terminus and N-terminus tagged constructs using HEK-293T cells was unsuccessful. Transfection efficiency of strumpellin in Cos-7 cell lines varied from 10% to 15%, but only N-terminus tagging was successful in a reproducible detection of expressed strumpellin, while C-terminus tagging resulted in very inconsistent levels of expressed strumpellin. This made it somewhat difficult to analyze the interactions of expressed WT and mutant forms of proteins. However, we first determined whether the expression of N-terminus-tagged strumpellin affected its trafficking and subcellular localization. We did not observe any detectable difference in the pattern of expression between endogenous strumpellin in cultured cortical rat neurons and expressed N-tagged strumpellin (Fig. 3A). This is in agreement with previously published data because Clemen et al also utilized N-tagging of strumpellin and did not report any alterations of its intracellular trafficking.[20]

Coexpression of WT eGFP:strumpellin and full-length spartin:myc in cos-7 cells (Fig. 3, upper row, panel C) showed a strong overlap in the subcellular distribution of these two proteins. The colocalization was more pronounced at the early endosomal compartment (Fig. 3B, only WT strumpellin shown), and this is in agreement with previous studies.[14,15,21]

Introduction of two studied strumpellin HSP-causing mutations N471D and V629F resulted in their abnormal

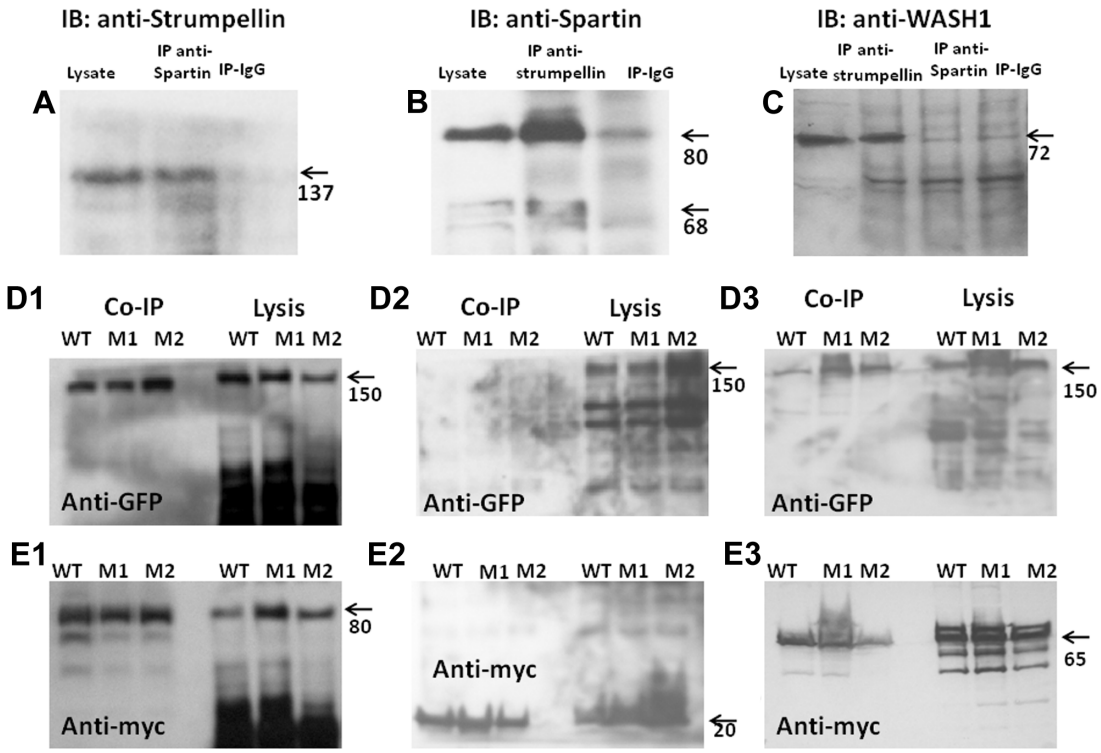

Figure 2. Strumpellin interacts with spartin. (**A**) Immunoprecipitation of the whole rat brain extracts proteins with spartin antibodies and analyzed by immunoblotting with strumpellin antibodies. (**B**) Immunoprecipitation with strumpellin antibodies and immunoblotted with spartin antibodies. First lanes show the studied proteins from cell lysates used for immunoprecipitation experiments, second lanes show antibodies used as the "bait" (spartin panel A, strumpellin panel B) incubated with protein A/G, and third lanes show control experiments with protein A/G alone. The 137-kD band represents a full-length strumpellin, and the 80-kD band with an additional faint 68-kD band corresponds to spartin. Very faint bands were also present in lanes Ip-IgG in panels A-1 and B, representing a nonspecific background; however, lanes IP anti-strumpellin and IP anti-spartin with co-immunoprecipitation had more than 100-fold higher activity in both instances. (**C**) Immunoprecipitation of WASH1 protein with strumpellin antibodies (second lane) and not by spartin antibodies (third lane). A faint nonspecific band was detected in control experiments without addition of specific antibodies (panel C, fourth lane). Panels D1–3 and E1–3 show interactions of WT and studied strumpellin mutations with a full-length spartin and spartin fragments 1–208 and 208–666. All three forms of expressed strumpellin:GFP, WT (lanes 1), N471D mutation (M1, lanes 2) and V629F (M2, lanes 3) interacted with a full length of spartin:myc (panel D1 spartin bait, panel E1 strumpellin bait). Coexpression of strumpellin:GFP and spartin:myc 1–208 did not pull down strumpellin:GFP (panel D2 spartin bait, panel E2 strumpellin bait) but the presence of spartin:myc 208–666 detected all three forms of strumpellin:GFP (panel D3 spartin bait, panel E3 strumpellin bait).

distribution when compared to a WT protein. Mutant forms of strumpellin were relatively absent in the cell periphery in heterologous cells, resulting in a clumpy expression, especially in the periventricular region (Fig. 3, second and third row, panel C). Coexpressed full-length spartin also strongly colocalized with mutant forms of strumpellin but there was no obvious redistribution of spartin in the presence of mutant forms of strumpellin.

Interaction between strumpellin and spartin is not affected by HSP-causing strumpellin mutations and does not require the MIT spartin domain. Using anti-GFP antibodies for eGFP:strumpellin and anti-myc antibodies for spartin:myc detection expressed in heterologous Cos-7 cells, we were able to replicate immunoprecipitation experiments assaying endogenous proteins in rat brain in spite of a relatively low rate of successful transfection (Fig. 2, panel D1 immunoprecipitation with anti-GFP and spartin as bait, panel E1 immunoprecipitation with anti-myc and strumpellin as bait). We also compared the interactions of WT strumpellin (lanes 1), N471D strumpellin (M1, lanes 2), and V629F (M2, lanes 3) with the full-length spartin (Fig. 2D1 and E1). This interaction was not altered by the presence of both studied HSP-causing mutations, and the overall affinity of mutant strumpellin forms and spartin did not differ from the WT form of strumpellin.

Spartin contains several conserved domains, including the MIT domain in the N-amino terminal region of the protein and a C-terminal plant-senescence related region.[11] We compared interactions of eGFP:strumpellin with spartin 1–208:myc (MIT domain) and spartin 208–666:myc containing the plant senescence region. The 1–208 fragment of spartin did not co-immunoprecipitate with strumpellin (Fig. 2D2 and E2), while all three forms of strumpellin [WT lanes 1, N471D (M1) lanes 2 and V629F (M2) lanes 3] co-immunoprecipitated with the 208–666 segment of spartin (Fig. 2D3 and E3). We could not fully assess the role

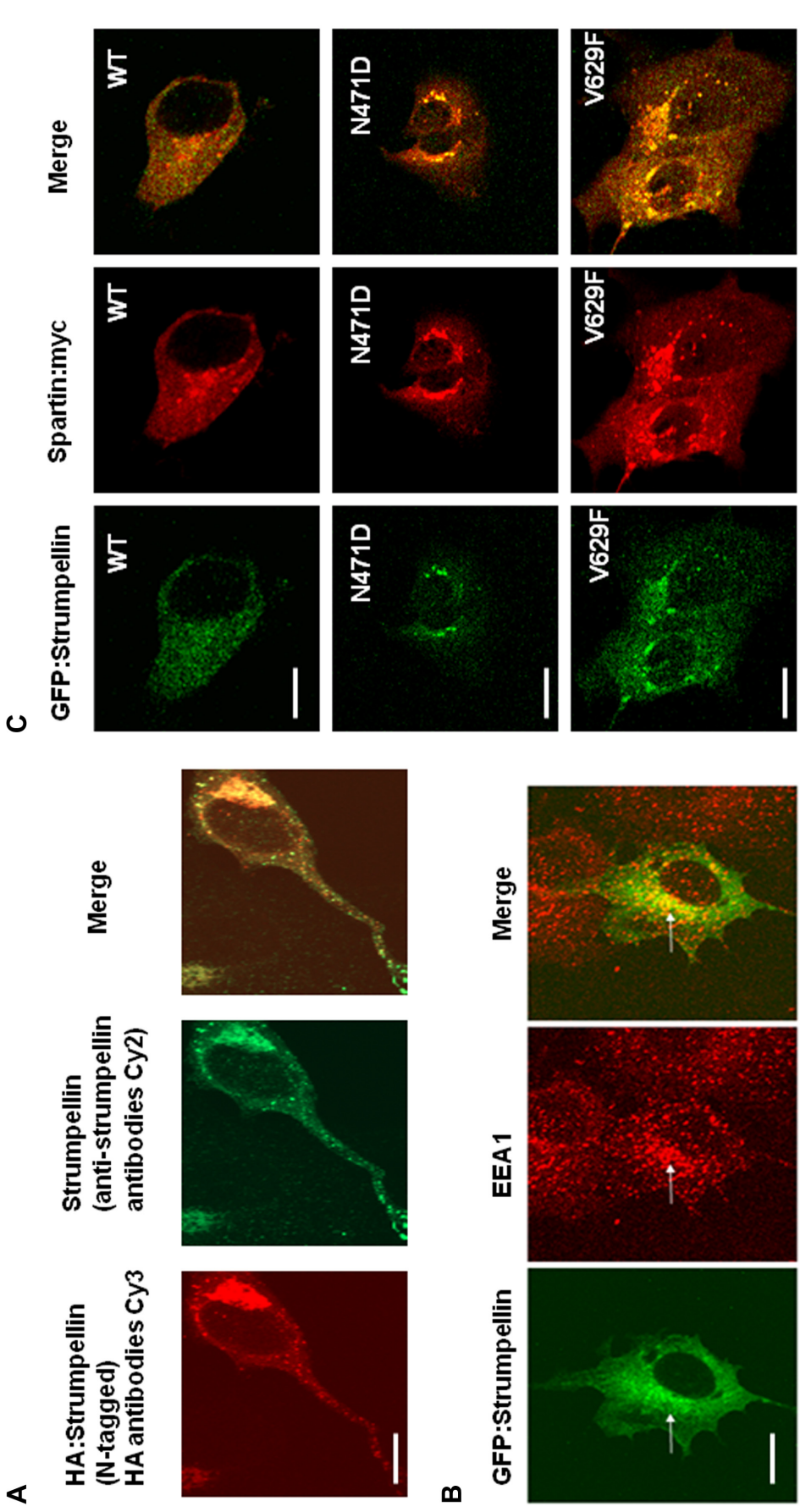

Figure 3. Overexpressed strumpellin and spartin colocalize. (**A**) Expressed N-tagged HA:strumpellin with the same subcellular localization as endogenous strumpellin in transfected cultured rat neurons. (**B**) Colocalization of WT overexpressed strumpellin with the early endosome antigen 1 (arrow). (**C**) (upper row) Coexpression of WT strumpellin:eGFP and full length (FL) spartin:myc in cos-7 cells; (middle row) coexpression of N471D strumpellin and FL spartin; and (bottom row) V629F strumpellin and FL spartin. Scale bar = 10 µm.

of the MIT domain for this interaction, but the 208–666 protein segment containing plant-related region within the C-terminus of spartin appears to play an important role in its binding to strumpellin.

Immunocytochemistry essentially confirmed the co-immunoprecipitation experiments that detected interactions of strumpellin with a full-length and 208–666 spartin. Spartin 1–208 had predominantly nuclear expression and did not colocalize with cytoplasmic WT or mutant forms of strumpellin (Fig. 4A). In contrast, spartin 208–666 showed almost exclusive colocalization with WT and mutant forms of strumpellin (Fig. 4B). Furthermore, the presence of spartin 208–666 also dramatically altered the pattern of subcellular distribution of WT strumpellin that formed aggregates in the cytoplasm very similar to those observed with HSP-causing forms of strumpellin.

Knockdown of endogenous strumpellin reduces neuronal branching and downregulates expression of endogenous spartin. Neurons expressing shRNA-targeting strumpellin demonstrated a nearly complete absence of this protein, as demonstrated by western blot of neuronal cells selected by flow cytometry (Fig. 5, first row of panel C and D, lane 2). Neurons expressing shRNA-targeting strumpellin exhibited a severe reduction of neuronal branching (Fig. 5F; $P < 0.01$). We have also noticed that neurons expressing shRNA-disrupting strumpellin had markedly reduced staining for endogenous spartin, while nontransfected neurons did not exhibit any obvious alterations of spartin expression (Fig. 5A and B). This observation was quantitatively confirmed by western blot from flow-cytometry-sorted cells, and neurons with knockdown of strumpellin had approximately 70% reduction of spartin levels (Fig. 5C and E; $P < 0.01$). Knockdown of strumpellin also affected the expression of WASH1 protein with approximate 40% reduction of its levels in neurons (Fig. 5C and E; $P < 0.05$). We also explored possible mechanisms of reduced expression of spartin. Quantitative RT-PCR did not detect any differences in mRNA levels (data not shown), arguing against interference with transcription and supporting that the reduced amount of spartin protein might be due accelerated protein degradation. We confirmed this mechanism by proteosomal inhibition of transfected neurons before their harvesting. The treatment of these cells with the MG-132 proteosome inhibitor stabilized the levels of spartin and WASH1 proteins (Fig. 5D).

The reverse experiments with knockdown expression of spartin did not affect the expression levels of endogenous strumpellin in neurons. Similarly, WASH1 levels were also unchanged (Fig. 6A and C). We also semiquantitatively assessed the neuronal branching after spartin RNAi using the most effective shRNA construct targeting spartin. We did not observe any statistically significant differences between the degrees of neuronal outgrowth 2 and 14 days after transfection; however, these neurons showed a tendency toward increased branching, which was also reported in knockout mouse (Fig. 6B and D).[16]

Discussion

The pathogenesis of SPG8, caused by mutations in the *KIAA0196* gene, is only emerging. Strumpellin is a member of the WASH complex, and knockdown expression of other members of this complex such as SWIP/KIAA1033, WASH1, or FAM21 caused increased tubulation of early endosomes with their abnormal trafficking.[21,22] However, no obvious WASH complex abnormalities were observed in neurons expressing mutant forms of strumpellin.[8] Several HSP-causing genes encode proteins important for the endosomal trafficking and sorting processes.[1,2] This suggests that shared biochemical pathways are responsible for selective axonal degeneration. Direct biochemical interactions between several HSP-associated proteins have been reported, including atlastin-1/spastin, spastin/REEP1, REEP1/atlastin-1, and NIPA1/atlastin-1.[17,23–25]

Our data suggest that spartin/strumpellin interactions take place outside of the WASH complex because we could not co-immunoprecipitate spartin and WASH1 proteins. Furthermore, spartin was never suggested as a putative member of this protein complex. Possible interactions of spartin with other known proteins from this complex need to be carefully explored, but our data support additional functions for strumpellin not requiring the interactions with other members of the WASH complex. Spartin is ubiquitously expressed and colocalizes with early endosomes.[10] It likely serves as a multifunctional protein, including an ubiquitin ligase interacting protein important for the regulation of lipid droplet biogenesis by promoting AIP4-mediated ubiquitination of several lipid droplet proteins, epidermal growth factor receptor trafficking, and an inhibitor of the bone morphogenic signaling pathway.[14–16,26] It remains unknown which of these functions are crucial for the pathogenesis of HSP. Our data do not provide any additional insights into the biochemical pathway requiring the interaction of strumpellin and spartin. We did not include the specific truncated form of spartin associated with Troyer syndrome in our experiments because truncated transcripts undergo nonsense-mediated decay with a loss-of-function mechanism of axonal degeneration.[19] Thus, our experiments with knockdown of spartin should closely reflect intracellular levels of spartin in individuals with Troyer syndrome. We did not detect any obvious changes in strumpellin expression under these circumstances. However, mutant forms of strumpellin altered the intracellular distribution of spartin, suggesting the disruption of normal function of spartin in SPG8. Previously identified cellular functions of spartin are also important candidate mechanisms for strumpellin functions outside the WASH1 complex. It is also intriguing that the segment of spartin containing plant-related senescence rather than the MIT domain was critical for the binding of strumpellin. Spartin binds to mitochondrial outer membrane via the plant-related senescence (PRS) domain, and it was proposed that this regulates mitochondrial calcium uptake.[13,27]

We identified the second biochemical interaction of strumpellin that is putatively outside the WASH complex.

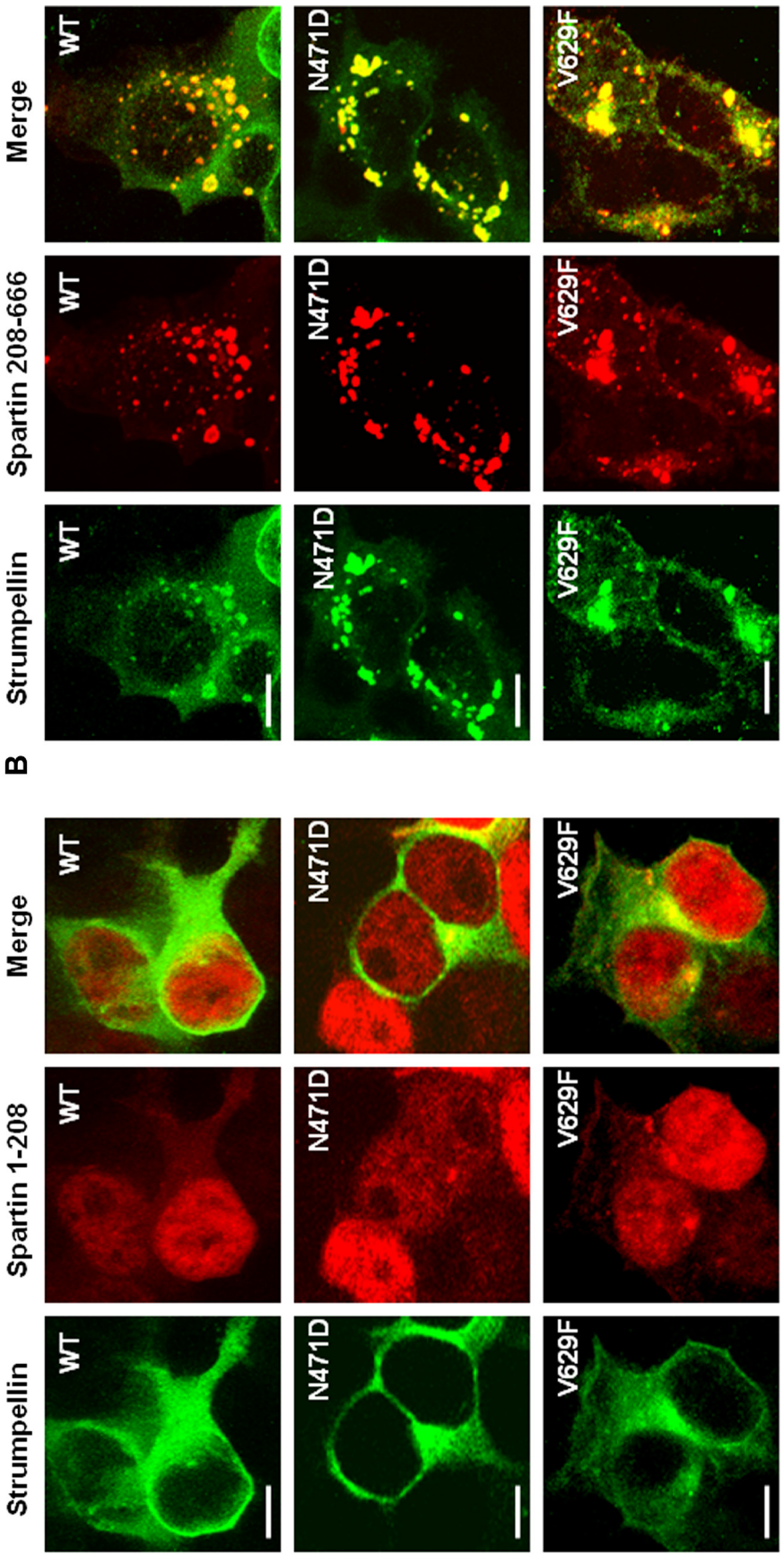

Figure 4. Overexpressed spartin 208–666 alters the intracellular distribution of strumpellin. (**A**) Spartin 1–208 with predominantly nuclear expression. Colocalization with WT or mutant forms of strumpellin was not observed. (**B**) Spartin 208–666 with almost exclusive colocalization with WT and mutant forms of strumpellin. Scale bar = 10 µm.

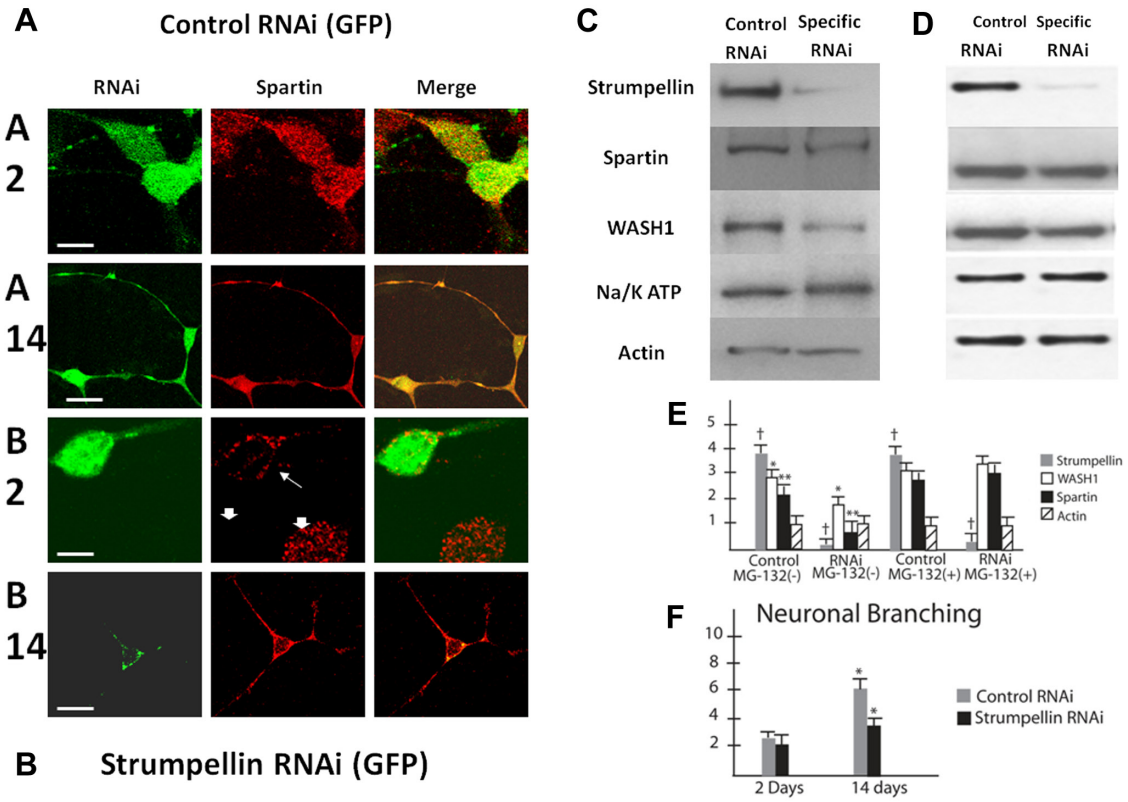

Figure 5. Knockdown of strumpellin reduces the level of endogenous spartin. (**A**) Rat cortical neurons expressing control (scrambled nonsensical) shRNA with normal branching and endogenous levels of spartin at day 2 (A2) and day 14 (A14). (**B**) Knockdown of strumpellin with reduced endogenous spartin staining (long arrows designate neurons expressing shRNA targeting strumpellin as indicated by GFP expression) when compared to neurons that were not transfected with this RNAi construct (short arrows) at day 2 (B2) and day 14 (B14). (**C**) Western blotting of strumpellin, spartin, and WASH1 levels from rat neurons targeted for strumpellin knockdown (lane 1 control RNAi, lane 2 RNAi of strumpellin). (**D**) The same experiment after treatment with MG-132. Actin and sodium/potassium ATPase were used as loading controls. (**E**) Plotting of expression levels of strumpellin, spartin, and WASH1 proteins normalized to actin levels (shown as value 1 on *y*-axis) from experiments shown on panels C and D. (**E**) Semiquantitative analysis of neuronal branching assessed after 2 and 14 days. The *y*-axis shows the sum of counted primary and secondary branching. Scale bar = 5 μm.
Notes: *$p < 0.01$, *$p < 0.05$, **$p < 0.01$, †$p < 0.001$.

Strumpellin also colocalizes with the valosin-containing protein (VCP).[20] VPC is a multifunctional protein and mutations in this gene most commonly cause inclusion body myopathy with Paget disease or amyotrophic lateral sclerosis associated with frontotemporal dementia.[28] Recently, a novel VCP mutation has been identified as a cause of HSP as well.[29] However, there is no evidence that VCP is a part of the WASH complex, further supporting additional roles of strumpellin outside the WASH complex.[20]

Conclusion

We present three different types of evidence supporting that strumpellin and spartin are interacting partners, including co-immunoprecipitation of both endogenous and overexpressed forms of proteins, immunocytologic colocalization in both heterologous and neuronal cell types, and significant alterations in spartin expression in strumpellin knockdown conditions. All identified HSP-causing mutations in strumpellin are missense, and both mutant and WT are expected to be present in equal amounts in cells expressing this protein. Thus, knockdown of strumpellin with subsequent spartin level reduction is not an expected physiologic situation playing a role in the pathogenesis of HSP, but it further strengthens our observations that these two proteins are indeed interacting. Several published studies of the WASH complex have reported that the individual protein components of the WASH complex are interdependent for their stability. The knock down of SWIP/KIAA1033 protein markedly reduces the levels of endogenous strumpellin.[7,30] We observed a similar phenomenon with lower expression levels of WASH1 protein induced by knockdown of strumpellin, and this was reversed by proteosome inhibition. Even though we propose that the interaction between spartin and strumpellin is not a part of the WASH complex, this result supports the interaction of these two proteins.

Our report is the first study showing the binding of endogenous and overexpressed strumpellin and spartin. This suggests that the pathogenesis of HSP caused by mutation in these two proteins is fundamentally related, and provides additional evidence that HSP may be caused by abnormalities in proteins that are members of the same biochemical pathway. Further studies will hopefully elucidate the role of

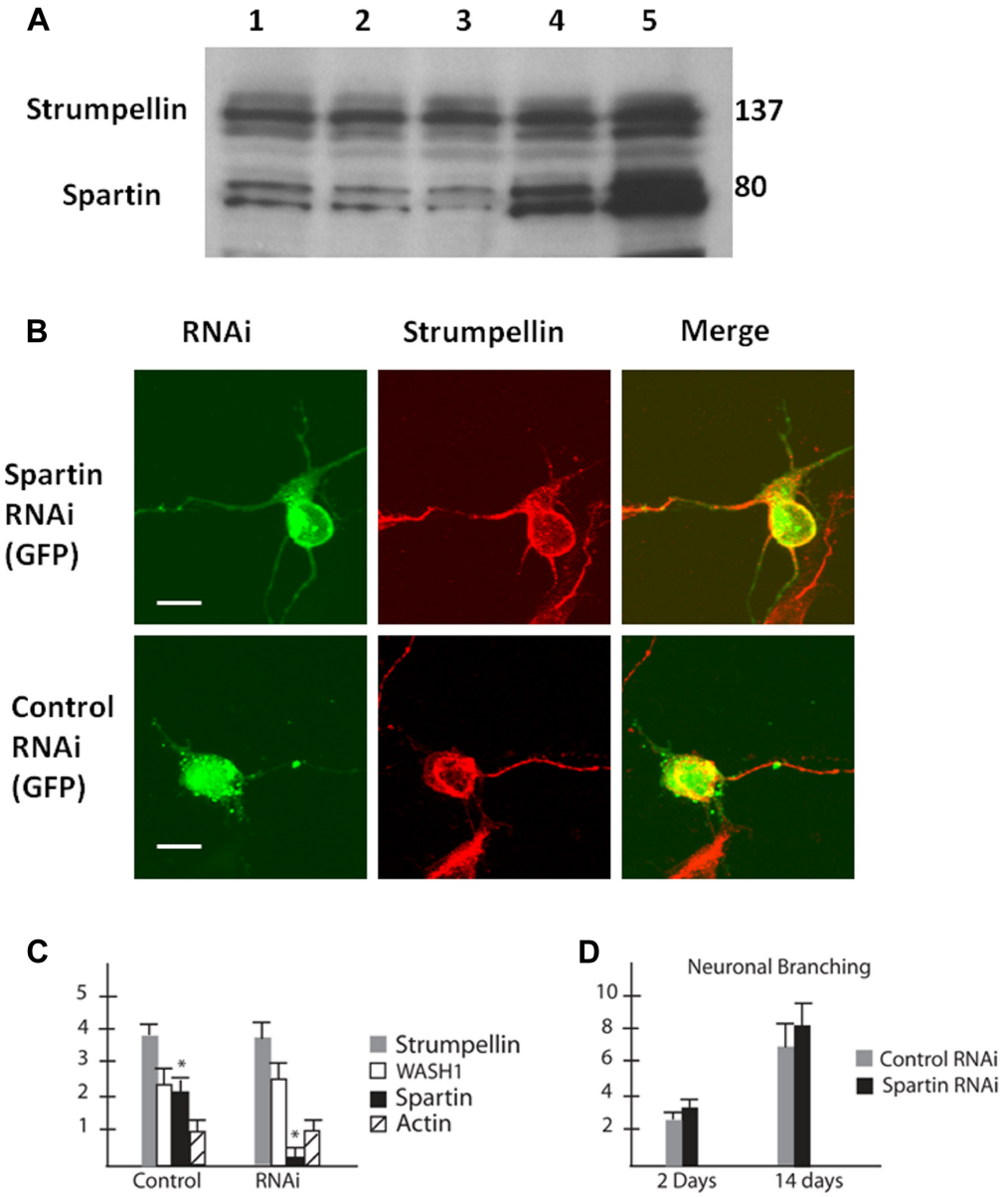

Figure 6. Knock-down of spartin did not alter endogenous strumpellin expression. (**A**) Western blotting of spartin after four different constructs targeting rat spartin were tested (lanes 1–4 correspond to four anti-spartin constructs and the fifth lane to a control, nonsensical RNA). (**B**) Rat cortical neurons expressing shRNA targeting spartin (construct #3) without any changes in endogenous strumpellin levels. (**C**) Plot of the expression levels of strumpellin, spartin, and WASH1 proteins normalized to actin levels (shown as value 1 on *y*-axis). (**D**) Semiquantitative analysis of neuronal branching assessed after 2 and 14 days. The *y*-axis shows the sum of counted primary and secondary branching, and the observed difference was not statistically significant. Scale bar = 5 μm.
Note: *$p < 0.001$.

this interaction in axonal maintenance and consequences of HSP-causing mutations leading to axonal degeneration.

Acknowledgment

We gratefully acknowledge the use of the Vanderbilt University Medical Center Cell Imaging Core Resource, which is supported by National Institutes of Health Grants CA68485 and DK20593.

Author Contributions

Conceived and designed the experiments: JZ, PH. Analyzed the data: PH. Wrote the first draft of the manuscript: PH. Contributed to the writing of the manuscript: JZ. Agree with manuscript results and conclusions: JZ, PH. Jointly developed the structure and arguments for the paper: JZ, PH. Made critical revisions and approved final version: JZ, PH. Both authors reviewed and approved of the final manuscript.

REFERENCES

1. Blackstone C, O'Kane CJ, Reid E. Hereditary spastic paraplegias: membrane traffic and the motor pathway. *Nat Rev Neurosci*. 2011;12(2):31–42.
2. Blackstone C. Cellular pathways of hereditary spastic paraplegia. *Annu Rev Neurosci*. 2012;35:25–47.

3. Finsterer J, Löscher W, Quasthoff S, Wanschitz J, Auer-Grumbach M, Stevanin G. Hereditary spastic paraplegias with autosomal dominant, recessive, X-linked, or maternal trait of inheritance. *J Neurol Sci*. 2012;318(1–2):1–18.
4. Fink JK, Hedera P. Hereditary spastic paraplegia: genetic heterogeneity and genotype-phenotype correlation. *Semin Neurol*. 1999;19(3):301–309.
5. Hedera P, DiMauro S, Bonilla E, Wald J, Eldevik OP, Fink JK. Phenotypic analysis of autosomal dominant hereditary spastic paraplegia linked to chromosome 8q. *Neurology*. 1999;53(1):44–50.
6. Valdmanis PN, Meijer IA, Reynolds A, et al. Mutations in the KIAA0196 gene at the SPG8 locus cause hereditary spastic paraplegia. *Am J Hum Genet*. 2007; 80(1):152–161.
7. Jia D, Gomez TS, Metlagel Z, et al. WASH and WAVE actin regulators of the Wiskott-Aldrich syndrome protein (WASP) family are controlled by analogous structurally related complexes. *Proc Natl Acad Sci U S A*. 2010;107(23): 10442–10447.
8. Freeman C, Seaman MN, Reid E. The hereditary spastic paraplegia protein strumpellin: characterization in neurons and of the effect of disease mutations on WASH complex assembly and function. *Biochim Biophys Acta*. 2013;1832(1): 160–173.
9. Proukakis C, Cross H, Patel H, Patton MA, Valentine A, Crosby AH. Troyer syndrome revisited. A clinical and radiological study of a complicated hereditary spastic paraplegia. *J Neurol*. 2004;251(9):1105–1110.
10. Robay D, Patel H, Simpson MA, Brown NA, Crosby AH. Endogenous spartin, mutated in hereditary spastic paraplegia, has a complex subcellular localization suggesting diverse roles in neurons. *Exp Cell Res*. 2006;312(15):2764–2777.
11. Patel H, Cross H, Proukakis C, et al. SPG20 is mutated in Troyer syndrome, an hereditary spastic paraplegia. *Nat Genet*. 2002;31(4):347–348.
12. Ciccarelli FD, Proukakis C, Patel H, et al. The identification of a conserved domain in both spartin and spastin, mutated in hereditary spastic paraplegia. *Genomics*. 2003;81(4):437–441.
13. Joshi DC, Bakowska JC. SPG20 protein spartin associates with cardiolipin via its plant-related senescence domain and regulates mitochondrial Ca2+ homeostasis. *PLoS One*. 2011;6(4):e19290.
14. Bakowska JC, Jupille H, Fatheddin P, Puertollano R, Blackstone C. Troyer syndrome protein spartin is mono-ubiquitinated and functions in EGF receptor trafficking. *Mol Biol Cell*. 2007;18(5):1683–1692.
15. Edwards TL, Clowes VE, Tsang HT, et al. Endogenous spartin (SPG20) is recruited to endosomes and lipid droplets and interacts with the ubiquitin E3 ligases AIP4 and AIP5. *Biochem J*. 2009;423(1):31–39.
16. Renvoisé B, Stadler J, Singh R, Bakowska JC, Blackstone C. Spg20-/- mice reveal multimodal functions for Troyer syndrome protein spartin in lipid droplet maintenance, cytokinesis and BMP signaling. *Hum Mol Genet*. 2012;21(16): 3604–3618.
17. Botzolakis EJ, Zhao J, Gurba KN, MacDonald RL, Hedera P. The effect of HSP-causing mutations in SPG3A and NIPA1 on the assembly, trafficking, and interaction between atlastin-1 and NIPA1. *Mol Cell Neurosci*. 2001;46(1):122–135.
18. Zhao J, Hedera P. Hereditary spastic paraplegia-causing mutations in atlastin-1 interfere with BMPRII trafficking. *Mol Cell Neurosci*. 2013;52(1):87–96.
19. Bakowska JC, Wang H, Xin B, Sumner CJ, Blackstone C. Lack of spartin protein in Troyer syndrome: a loss-of-function disease mechanism? *Arch Neurol*. 2008;65(4):520–524.
20. Clemen CS, Tangavelou K, Strucksberg KH, et al. Strumpellin is a novel valosin-containing protein binding partner linking hereditary spastic paraplegia to protein aggregation diseases. *Brain*. 2010;133(10):2920–2941.
21. Harbour ME, Breusegem SY, Antrobus R, Freeman C, Reid E, Seaman MN. The cargo-selective retromer complex is a recruiting hub for protein complexes that regulate endosomal tubule dynamics. *J Cell Sci*. 2010;123(21):3703–3717.
22. Derivery E, Sousa C, Gautier JJ, Lombard B, Loew D, Gautreau A. The Arp2/3 activator WASH controls the fission of endosomes through a large multiprotein complex. *Dev Cell*. 2009;17(5):712–723.
23. Evans K, Keller C, Pavur K, Glasgow K, Conn B, Lauring B. Interaction of two hereditary spastic paraplegia gene products, spastin and atlastin, suggests a common pathway for axonal maintenance. *PNAS*. 2006;103(28):10666–10671.
24. Sanderson CM, Connell JW, Edwards TL, et al. Spastin and atlastin, two proteins mutated in autosomal dominant hereditary spastic paraplegia, are binding partners. *Hum Mol Genet*. 2006;5(2):307–318.
25. Park SH, Zhu PP, Parker RL, Blackstone C. Hereditary spastic paraplegia proteins REEP1, spastin, and atlastin-1 coordinate microtubule interactions with the tubular ER network. *J Clin Invest*. 2010;120(4):1097–1110.
26. Tsang HT, Edwards TL, Wang X, et al. The hereditary spastic paraplegia proteins NIPA1, spastin and spartin are inhibitors of mammalian BMP signaling. *Hum Mol Genet*. 2009;18(20):3805–3821.
27. Lu J, Rashid F, Byrne PC. The hereditary spastic paraplegia protein spartin localises to mitochondria. *J Neurochem*. 2006;98(6):1908–1919.
28. Watts GD, Wymer J, Kovach MJ, et al. Inclusion body myopathy associated with Paget disease of bone and frontotemporal dementia is caused by mutant valosin-containing protein. *Nat Genet*. 2004;36(4):377–381.
29. de Bot ST, Schelhaas HJ, Kamsteeg EJ, van de Warrenburg BP. Hereditary spastic paraplegia caused by a mutation in the VCP gene. *Brain*. 2012;135(12):e224.
30. Ropers F, Derivery E, Hu H, et al. Identification of a novel candidate gene for non-syndromic autosomal recessive intellectual disability: the WASH complex member SWIP. *Hum Mol Genet*. 2011;20(13):2585–2590.